

Proceeding Series of the Brazilian Society of Computational and Applied Mathematics

Two dimensional hierarchical mixed finite element approximations with enhanced primal variable accuracy

Agnaldo M. Farias¹

Departamento de Matemática, IFNMG, Salinas, MG

Philippe R. B. Devloo²

Departamento de Estruturas, FEC-Unicamp, Campinas, SP

Sônia M. Gomes³

Departamento de Matemática Aplicada, IMECC-Unicamp, Campinas, SP

Denise de Siqueira⁴

Departamento de Matemática, UTFPR, Curitiba, PR

Douglas A. Castro⁵

Universidade Federal do Tocantins, Campus Gurupi, TO

Abstract. The purpose of the present paper is to analyse different possibilities of choosing balanced pairs of approximation spaces for dual (flux) and primal (pressure) variables to be used in discrete versions of the mixed finite element method for affine two dimensional meshes. In all space configurations, the principle guiding their construction is the property that the divergence of the dual space and the primal approximation space should coincide, while keeping the same order of accuracy for the flux variable and varying the accuracy order of the primal variable. There is the classic case of BDM_k spaces based on triangular meshes and polynomials of total degree k for the dual variable, and $k - 1$ for the primal variable, showing stable simulations with optimal convergence rates of orders $k + 1$ and k , respectively. Another case is related to RT_k and $BDFM_{k+1}$ spaces for quadrilateral and triangular meshes, respectively. It gives identical approximation order $k + 1$ for both primal and dual variables, an improvement in accuracy obtained by increasing the degree of primal functions to k , and by enriching the dual space with some properly chosen internal shape functions of degree $k + 1$, while keeping degree k for the border fluxes. A new type of approximation is proposed by further incrementing the order of some internal flux functions to $k + 2$, and matching primal functions to $k + 1$ (higher than the border fluxes of degree k). Thus, higher convergence rate of order $k + 2$ is obtained for the primal variable. Using static condensation, the global condensed system to be solved in all the cases have same dimension (and structure), which is proportional to the space dimension of the border fluxes for each element geometry.

Keywords. Finite elements, $\mathbf{H}(\text{div})$ spaces, mixed formulation, approximation space configurations, convergence rates.

¹agnaldo.farias@ifnmg.edu.br

²phil@fec.unicamp.br

³soniag@ime.unicamp.br

⁴denisesiqueira@utfpr.edu.br

⁵dacastro@mail.uft.edu.br

1 Introduction

Mixed finite element methods have the ability to provide accurate and locally conservative fluxes, an advantage over standard H^1 finite element discretizations [4]. They are based on simultaneous approximations of the primal (pressure) and dual (flux) variables, involving two kinds of approximation spaces. $\mathbf{H}(\text{div})$ -conforming approximation spaces are used for the dual variable, with continuous normal components over element interfaces, and the primal variable is usually represented in discontinuous finite element spaces.

Since the pioneering work by Raviart and Thomas [6] in 1977, different constructions of $\mathbf{H}(\text{div})$ approximation spaces have been proposed in [2, 3, 5]. Recently, several other papers have appeared in the literature due to increasing interest on this subject [1, 7].

The main purpose of this article is to analyse different ways of choosing balanced pairs of approximation spaces (\mathbf{V}_h, U_h) , for dual and for primal variables, based on affine triangular and quadrilateral meshes, to be used in discrete versions of the mixed finite element method for two dimensional elliptic problems. The methods share the following basic characteristics:

1. The flux approximation spaces \mathbf{V}_h are spanned by a hierarchy of vectorial shape functions, which are organized into two classes: the shape functions of interior type, with vanishing normal components over all element edges, and the shape functions associated to the element edges.
2. In all the cases, the commutation De Rham property holds. Specifically,

$$\nabla \cdot \mathbf{V}_h = U_h, \quad (1)$$

implying stable simulations with optimal L^2 -error convergence orders, which are dictated by the degree of the complete set of polynomials used in the approximations.

All the implementations of the present paper are performed in the object-oriented scientific computational environment NeopZ⁶. This is a general finite element approximation software organized by modules for a broad classes of technologies, incorporating a variety of element geometries, variational formulations, and approximation spaces.

The paper is organized as follows. The mixed element formulation for an elliptic model problem is set in Section 2. The proposed approximation space configurations are described in Section 3, where the static condensation strategy is stated for them. The results of the applications of these approximation spaces on discrete formulations of a model problem are discussed in Section 4. Section 5 gives the final conclusions of the article.

2 Mixed finite element method for a model problem

Consider a model Poisson problem expressed as:

$$\begin{aligned} \boldsymbol{\sigma} &= -\nabla u \quad \text{in } \Omega, \\ \nabla \cdot \boldsymbol{\sigma} &= f \quad \text{in } \Omega, \\ u &= 0 \quad \text{in } \partial\Omega, \end{aligned}$$

⁶<http://github.com/labmec/neopz>

where $\Omega \subset \mathbb{R}^2$ is the computational domain with Lipschitz boundary $\partial\Omega$. As studied in [4], the classical mixed formulation for this problem requires the space

$$\mathbf{H}(\text{div}, \Omega) = \left\{ \mathbf{q} \in [L^2(\Omega)]^2; \nabla \cdot \mathbf{q} \in L^2(\Omega) \right\},$$

and to find $(\boldsymbol{\sigma}, u) \in \mathbf{V} \times U = \mathbf{H}(\text{div}, \Omega) \times L^2(\Omega)$ such that

$$a(\boldsymbol{\sigma}, \mathbf{q}) + b(\mathbf{q}, u) = 0, \tag{2}$$

$$b(\boldsymbol{\sigma}, \varphi) = \ell(\varphi), \tag{3}$$

where $a(\boldsymbol{\sigma}, \mathbf{q}) = \int_{\Omega} \boldsymbol{\sigma} \cdot \mathbf{q} \, d\Omega$, $b(\mathbf{q}, u) = - \int_{\Omega} u \nabla \cdot \mathbf{q} \, d\Omega$, and $\ell(\varphi) = - \int_{\Omega} f \varphi \, d\Omega$.

In typical $\mathbf{H}(\text{div})$ -conforming discretized versions of the mixed formulation, approximate solutions for dual $\boldsymbol{\sigma}$ and primal u variables are searched in finite dimensional subspaces $\mathbf{V}_h \subset \mathbf{V}$ and $U_h \subset U$, and the system of variational equations (2)-(3) are enforced by test functions $\mathbf{q} \in \mathbf{V}_h$ and $\varphi \in U_h$.

3 Types of approximation space configurations

Three cases for the choice of approximation space configuration (\mathbf{V}_h, U_h) shall be considered. For their definitions, there are polynomial spaces P_k used in the construction of scalar approximations for the primal variable, where the index k refers to polynomial degree. For triangular, the polynomials in P_k have total degree k , and for quadrilateral, they have maximum degree k in each coordinate. Vectorial polynomial spaces \mathbf{P}_k mean that the components of the vectorial shape functions are obtained from polynomials in P_k .

Approximation space configuration of type $\mathbf{P}_k P_{k-1}$. For this configuration, the dual approximation space is of type \mathbf{P}_k , based on complete vector valued polynomials of degree k , and the primal approximation space P_{k-1} is based on the complete scalar valued polynomials of degree $k - 1$. However, this kind of space configuration satisfying property (1) can only be valid for triangular meshes, corresponding to the classic BDM_k elements [3], with L^2 -error convergence of orders $k + 1$ and k for dual and primal variables.

Approximation spaces of type $\mathbf{P}_k^* P_k$. For triangular and quadrilateral geometries, another type of space configuration can be considered. Guided by the verification of property (1), the dual approximations in \mathbf{V}_h are said to be of \mathbf{P}_k^* type if they are locally spanned by the face functions of \mathbf{P}_k type, and by the internal shape functions of \mathbf{P}_{k+1} defined by vectorial polynomials of degree $k + 1$ whose divergence are included in the primal approximation space of type P_k . Since the incomplete dual approximation space of type \mathbf{P}_k^* only involves the complete vector valued polynomials of degree k , in simulations using $\mathbf{P}_k^* P_k$ configurations the expected L^2 -error convergence rates are of order $k + 1$ for both dual and primal variables. This is the type of RT_k space configuration for quadrilateral geometries [6], and of $BDFM_{k+1}$ elements for triangular elements [2].

Approximation spaces of type $\mathbf{P}_k^{} P_{k+1}$.** This is a new space configuration, where the construction of dual approximation spaces of type \mathbf{P}_k^{**} consists in adding to the complete

vector valued spaces of type \mathbf{P}_k those interior shape functions of \mathbf{P}_{k+1}^* defined by vectorial polynomials of degree $k + 2$ whose divergence are included in the primal approximation space of type P_{k+1} . Therefore, in \mathbf{P}_k^{**} the face shape functions are still obtained by polynomials of degree $\leq k$, but some of the internal shape functions may be obtained from polynomials of degree up to $k + 2$. As in the previous case, here the verification of property (1) is the basic principle guiding the definition of the pair of approximation spaces. Since the spaces of type \mathbf{P}_k^{**} contains only the complete vector valued approximations of type \mathbf{P}_k , the L^2 -error convergence rate of order $k + 1$ is expected for the dual variable. However, for primal variable a higher order $k + 2$ of convergence may be reached.

Vectorial shape functions. For the numerical tests presented in the next section for affine partitions, flux approximations are expressed in terms of vectorial shape functions forming bases of type \mathbf{P}_k , \mathbf{P}_k^* and \mathbf{P}_k^{**} . The numbers of these vectorial shape functions are presented in Table 1. The methodology adopted here for their construction is an extension of previous developments in [7], where the principle is to choose appropriate constant vector fields, based on the geometry of each element of a given partition of the computational region Ω , which are multiplied by an available set of H^1 hierarchical scalar basic functions to obtain the vectorial shape functions.

Table 1: Number of vectorial shape functions in the bases of type \mathbf{P}_k , \mathbf{P}_k^* and \mathbf{P}_k^{**}

Element	Type	Edge	Internal	Total
Triangular	\mathbf{P}_k	$3(k + 1)$	$k^2 - 1$	$(k + 1)(k + 2)$
	\mathbf{P}_k^*	$3(k + 1)$	$(k + 1)^2 - 1$	$3 + k(k + 5)$
	\mathbf{P}_k^{**}	$3(k + 1)$	$(k + 1)^2 - 1$	$(k + 1)(k + 6)$
Quadrilateral	\mathbf{P}_k	$4(k + 1)$	$2(k^2 - 1)$	$2(k + 1)^2$
	\mathbf{P}_k^*	$4(k + 1)$	$2k(k + 1)$	$2(k + 1)(k + 2)$
	\mathbf{P}_k^{**}	$4(k + 1)$	$2(k + 1)(k + 2)$	$2(k + 1)(k + 4)$

Static condensation. When using these kinds of approximations in the mixed formulation, the degrees of freedom of the flux may be organized in the form σ_{ih} , σ_{eh} , where σ_{ih} and σ_{eh} refer to internal and edge components of the flux, respectively. For the pressure, a scalar value is denoted by u_{0h} , and u_{ih} are the values of the pressure approximation except u_{0h} . Thus, the system (2)-(3) may be represented in the matrix form

$$\left(\begin{array}{cc|cc} A_{ii} & B_{ii}^T & B_{ie}^T & A_{ie} \\ B_{ii} & 0 & 0 & B_{ie} \\ \hline B_{ie} & 0 & 0 & B_{ee} \\ A_{ei} & B_{ie}^T & B_{ee}^T & A_{ee} \end{array} \right) \begin{pmatrix} \sigma_{ih} \\ u_{ih} \\ u_{0h} \\ \sigma_{eh} \end{pmatrix} = \begin{pmatrix} 0 \\ -f_{ih} \\ -f_{0h} \\ 0 \end{pmatrix}.$$

Then, static condensation may be applied by eliminating the internal degrees of freedom σ_{ih} and u_{ih} , to get a condensed system in terms of σ_{eh} and u_{0h} . On each element, the dimension of the static condensed matrix is determined by the number of degrees of freedom of the face components σ_{eh} plus one, which coincides for the approximations spaces of types $\mathbf{P}_k P_{k-1}$, $\mathbf{P}_k^* P_k$ and $\mathbf{P}_k^{**} P_{k+1}$.

4 Numerical results

The adopted test problem is defined in $\Omega = (0, 1)^2$, and has exact solution $u(x, y) = \sin(\pi x) \sin(\pi y)$. Uniform quadrilateral meshes are considered with spacing $= 2^{-i}$, $i = 0, 1, \dots, 5$, and the triangular meshes are constructed from them by diagonal subdivision.

In the top side of Figure 1, the convergence curves are for triangular meshes, and the results are obtained with approximation spaces of type $\mathbf{P}_k P_{k-1}$ (dotted lines), $\mathbf{P}_k^* P_k$ (continuous lines), $\mathbf{P}_k^{**} P_{k+1}$ (dashed lines), for $k = 1$ (magenta lines), $k = 2$ (blue lines), $k = 3$ (red lines) and $k = 4$ (black lines). For the flux variable, optimal convergence rate $k+1$ occur for all the configurations. It is also noticeable that the $\mathbf{P}_k^* P_k$ and $\mathbf{P}_k^{**} P_k$ settings present very close flux error magnitudes, specially at the higher levels of refinement. For the primal variable, optimal convergence rates of orders k , $k+1$ and $k+2$ is verified for $\mathbf{P}_k P_{k-1}$, $\mathbf{P}_k^* P_k$, and $\mathbf{P}_k^{**} P_{k+1}$ type of spaces, respectively. It is also interesting to note that the pressure error curves using approximation spaces of the same order in primal variable almost coincide, independently of the type of approximation space used for the flux. For instance, the configurations $\mathbf{P}_4 P_3$, $\mathbf{P}_3^* P_3$, and $\mathbf{P}_2^{**} P_3$ give almost the same error magnitudes for the pressure, with quite different error magnitudes for the flux.

Using the uniform quadrilateral meshes, the L^2 -errors are presented in the bottom side of Figure 1 for approximation spaces of types $\mathbf{P}_k^* P_k$ (continuous lines), and $\mathbf{P}_k^{**} P_{k+1}$ (dashed lines). The expected optimal rates for dual and primal variables are obtained, and similar conclusions arise as in the triangular case.

The curves in Figure 2 illustrate the effectiveness of the static condensation procedure in the reduction of degrees of freedom in the mixed method. Using meshes with spacing $h = 1/32$, it can be observed that the efficiency is specially significant for higher accuracy levels. For instance, using triangular meshes, and $k = 4$, the percentages of condensed degrees of freedom are about 87%, 82% and 75% for the mixed method with configurations $\mathbf{P}_k^{**} P_{k+1}$, $\mathbf{P}_k^* P_k$, and $\mathbf{P}_k P_{k-1}$, respectively. Furthermore, it can also be observed that this gain in efficiency is more noticeable for quadrilateral elements, where these percentages are about 90%, and 86% for $\mathbf{P}_k^{**} P_{k+1}$, and $\mathbf{P}_k^* P_k$ configurations.

5 Conclusions

Different ways of choosing balanced pairs of finite element approximation spaces, based on triangular and quadrilateral meshes, are considered and compared for dual and primal variables for discrete versions of the mixed finite element method for affine meshes. Convergence studies are presented using families of hierarchical shape functions specially designed for affine meshes, which are constructed from polynomials of total degree k for triangle and of maximum degree k for quadrilateral elements.

For triangular meshes, there is the combination of spaces of type $\mathbf{P}_k P_{k-1}$. Other configurations denoted by $\mathbf{P}_k^* P_k$ and $\mathbf{P}_k^{**} P_{k+1}$ are analysed for triangular and quadrilateral geometries. The settings \mathbf{P}_k^* and \mathbf{P}_k^{**} are obtaining by enriching the complete flux space of type \mathbf{P}_k with some internal flux functions with degree up to $k+1$ or $k+2$, respectively. As expected, optimal rates in L^2 -norms for primal and dual variables are observed, which are

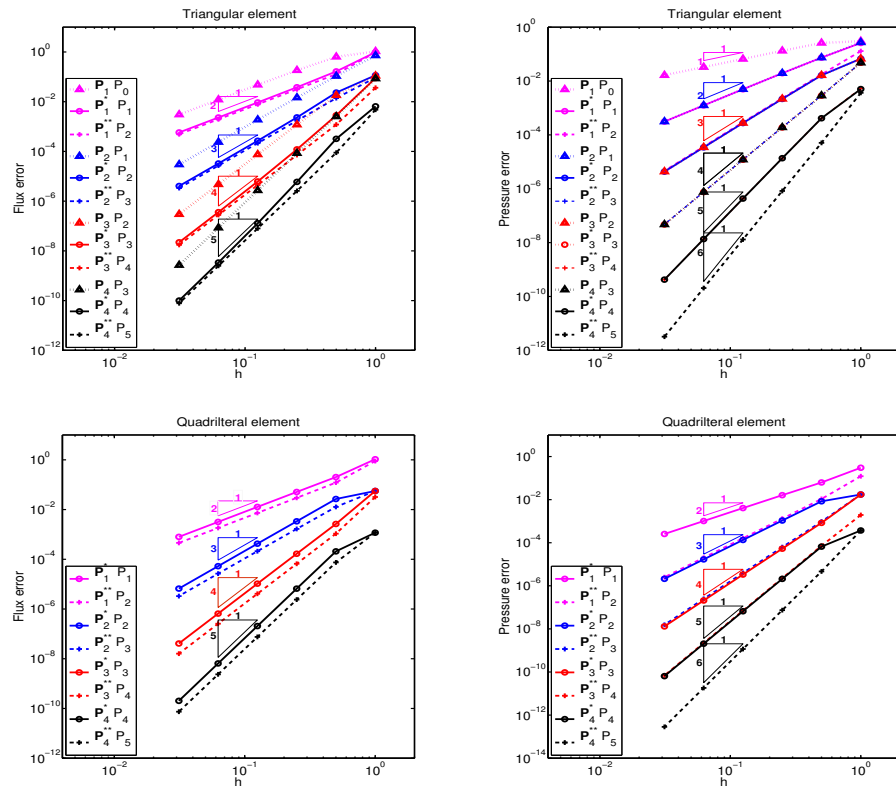


Figure 1: L^2 -errors for the flux (left side) and pressure (right side) versus h , with spaces of type $\mathbf{P}_k P_{k-1}$ (dotted), $\mathbf{P}_k^* P_k$ (continuous), and $\mathbf{P}_k^{**} P_{k+1}$ (dashed), for $k = 1$ (magenta), $k = 2$ (blue), $k = 3$ (red), and $k = 4$ (black) in the mixed formulation based on regular triangular meshes (top side), and quadrilateral meshes (bottom side).

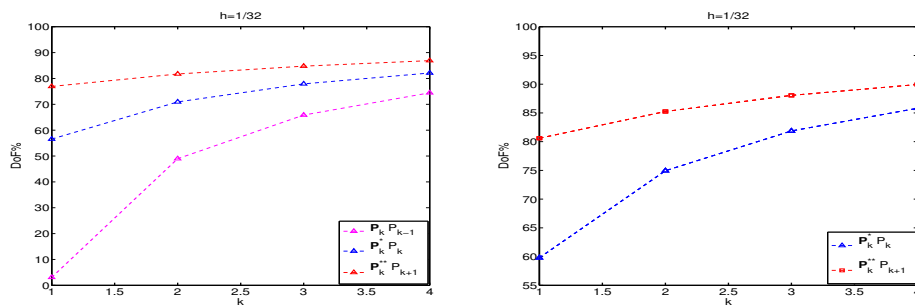


Figure 2: 2D model problem for triangular (left) and quadrilateral elements (right) with $h = 1/32$. Percentage of condensed degrees of freedom in the mixed formulation with spaces of type $\mathbf{P}_k^* P_k$ (blue), $\mathbf{P}_k^{**} P_{k+1}$ (red), and $\mathbf{P}_k P_{k-1}$ (magenta).

determined by the degree of the complete polynomial spaces included in the corresponding

approximations spaces.

In fact, the convergence rates of order $k + 1$ for the dual variable do not change by increasing the degrees of internal flux functions, as documented in \mathbf{P}_k^* and \mathbf{P}_k^{**} . But higher optimal convergence rates (i.e. $k + 1$ and $k + 2$) are obtained for the pressure variable when using the $\mathbf{P}_k^* P_k$ and $\mathbf{P}_k^{**} P_{k+1}$ function spaces, respectively, which are higher than the order k obtained when using the $\mathbf{P}_k P_{k-1}$ configuration. Because the meshes are affine, and $\nabla \cdot \boldsymbol{\sigma}_h$ results to be the $L^2(\Omega)$ -projection of $\nabla \cdot \boldsymbol{\sigma}$ on U_h , then the divergence error $\|\nabla \boldsymbol{\sigma} - \nabla \cdot \boldsymbol{\sigma}_h\|_{L^2(\Omega)}$ has the same accuracy rate as for the error in u .

In all three settings, the degrees of freedom associated with internal flux functions can be condensed, resulting in global matrices with identical sizes. For high order approximations, the number of condensed equations amounts to more than 80% of the total number of equations, which demonstrates the potential benefit of using $\mathbf{H}(\text{div})$ approximation spaces in parallel computers.

The authors are currently extending the methodology for three dimensional geometries, and for curved elements.

Acknowledgments. The author A. M. Farias thankfully acknowledges financial support received from FAPEMIG - Research Foundation of the State of Minas Gerais, Brazil. The authors P. R. B. Devloo and S. M. Gomes thankfully acknowledges financial support from ANP - Brazilian National Agency of Petroleum, Natural Gas, and Biofuels and the financial support from CNPq - Brazilian Research Council.

References

- [1] D. N. Arnold, D. Boffi, and R. S. Falk, Quadrilateral $\mathbf{H}(\text{div})$ finite elements, *SIAM J. Numer. Anal.*, 42 (6), 2429-2451, 2005.
- [2] F. Brezzi, J. Douglas, M. Fortin, L. D. Marini, Efficient rectangular mixed finite elements in two and three space variable, *RAIRO Modél. Math. Anal. Numér.*, 2, 581-604, 1987.
- [3] F. Brezzi, J. Douglas and L. D. Marini, Two Families of Mixed Finite Elements for Second Order Elliptic Problems, *Numer. Math.*, 47, 217-235, 1985.
- [4] F. Brezzi and M. Fortin, Mixed and Hybrid Finite Element Methods, *Springer Series in Computational Mathematics*, 15, Springer-Verlag, NewYork, 1991.
- [5] J. C. Nédélec, A New Family of Mixed Finite Elements in \mathbb{R}^3 , *Numer. Math.*, 50, 57-81, 1986.
- [6] P. A. Raviart and J. M. Thomas, A mixed finite element method for 2nd order elliptic problems, *Lect. Not. Math.*, 606, 292-315, 1997.
- [7] D. Siqueira, P. R. B. Devloo, S. M. Gomes. A new procedure for the construction of hierarchical high order $\mathbf{H}(\text{div})$ and $\mathbf{H}(\text{curl})$ finite element spaces, *Journal of Computational and Applied Mathematics*, 240, 204-214, 2013.